

10-22-2005

The catalytic reduction of NO by H₂ on Ru(0001): Observation of NHads species

A. Hornung

Ruhr-Universität Bochum, D-44780 Bochum, Germany

Dmitry Zemlyanov

Birck Nanotechnology Center, Purdue University, dimazemlyanov@purdue.edu

M. Muhler

Ruhr-Universität Bochum, D-44780 Bochum, Germany

G. Ertl

Fritz-Haber-Institut der Max-Planck-Gesellschaft, D-14195 Berlin, Germany

Follow this and additional works at: <http://docs.lib.purdue.edu/nanodocs>

Hornung, A.; Zemlyanov, Dmitry; Muhler, M.; and Ertl, G., "The catalytic reduction of NO by H₂ on Ru(0001): Observation of NHads species" (2005). *Other Nanotechnology Publications*. Paper 5.

<http://docs.lib.purdue.edu/nanodocs/5>

This document has been made available through Purdue e-Pubs, a service of the Purdue University Libraries. Please contact epubs@purdue.edu for additional information.

The catalytic reduction of NO by H₂ on Ru(0001): Observation of NH_{ads} species

A. Hornung^a, D. Zemlyanov^{b,*}, M. Muhler^a, G. Ertl^c

^a Ruhr-Universität Bochum, D-44780 Bochum, Germany

^b Materials and Surface Science Institute, Department of Physics, University of Limerick, Limerick, Ireland

^c Fritz-Haber-Institut der Max-Planck-Gesellschaft, D-14195 Berlin, Germany

Received 17 June 2005; accepted for publication 22 October 2005

Available online 5 December 2005

Abstract

Adsorption of NO and the reaction between NO and H₂ were investigated on the Ru(0001) surface by X-ray photoelectron spectroscopy (XPS). Surface composition was measured after NO adsorption and after the selective catalytic reduction of nitric oxide with hydrogen in steady-state conditions at 320 K and 390 K in a 30:1 mixture of H₂ and NO (total pressure = 10⁻⁴ mbar). After steady-state NO reduction, molecularly adsorbed NO in both the linear on-top and threefold coordinations, NH_{ads} and N_{ads} species were identified by XPS. The coverage of the NH_{ads} and N_{ads} species was higher after the reaction at 390 K than the corresponding values at 320 K. Strong destabilisation of N_{ads} by O_{ads} was detected. A possible reaction mechanism is discussed.
© 2005 Elsevier B.V. All rights reserved.

Keywords: X-ray photoelectron spectroscopy; Surface chemical reaction; Adsorption; Ruthenium; Nitrogen oxides; Low index single crystal surfaces; NO reduction; DeNOx

1. Introduction

Among the group VIII transition metals ruthenium is an object of particular interest because of its well-known catalytic activity towards several processes. In the synthesis of ammonia, it has found an industrial application in the Kellogg Advanced Ammonia Process (KAAP) [1,2], the selective catalytic reduction of nitrogen oxides [3,4], Fischer–Tropsch synthesis [5] and the hydrogenolysis of hydrocarbons [6]. The practical difficulties in the utilisation of Ru-based catalysts for the catalytic reduction of NO are connected with the formation of noxious volatile ruthenium oxides at high temperatures in the presence of gas phase oxygen. However, the remarkable selectivity of

ruthenium in NO reduction with hydrogen or ammonia to N₂ makes it an attractive object of study.

NO on the Ru(0001) surface has been subject of a number of theoretical and experimental studies [7–23], whereas less attention has been devoted to the reaction between H₂ and NO on ruthenium single crystals [11,24,25]. According to high-resolution energy electron loss spectroscopy (HREELS) and IR absorption spectroscopy (IRAS), below 200 K NO adsorbs molecularly either in threefold hollow and/or on-top positions [7,8,13,18]. Two NO stretching vibrations at approximately 1500 cm⁻¹, ν_1 , and 1800 cm⁻¹, ν_2 , were assigned to the threefold and on-top coordinated species, respectively. A detailed LEED-IV analysis [19,22] and a combined theoretical and experimental study by X-ray emission spectroscopy (XES) [21,23] showed the existence of three adsorption sites in the saturated NO_{ads} layer on Ru(0001). NO was found to adsorb on NO_{top}, NO_{hcp} and NO_{fcc} sites in upright orientations with the nitrogen end down. An N–O bond length for

* Corresponding author. Present address: Birck Nanotechnology Center (BRCK), Purdue University, 1205 West State Street, West Lafayette, IN 47907-2057, USA. Tel.: +1 765 4962457; fax: +1 765 4968383.

E-mail address: dimazemlyanov@purdue.edu (D. Zemlyanov).

the NO_{top} state is shorter than those for the bridge coordination [14,19,22]. The change of the N–O bond length agrees with the classic Blyholder model [26], according to which bonding of a NO molecule to a transition metal can be divided into σ donation and π back donation. As roughly estimated by a Mulliken population analysis [21], the adsorption complex in the hollow site experiences a substantially stronger back donation in comparison to the on-top site. The charge transfer at the hexagonal-close-packed (hcp) site is slightly higher than at the face-centred-cubic (fcc) site. Detailed discussion of the π back donation questions can be found elsewhere [21].

At room temperature and low coverage, NO dissociates completely on the Ru(0001) surface [9,17,20]. The dissociation takes place on the active sites with low coordination such as an atomic step [17]. The molecular adsorption states of NO, ν_1 and ν_2 , are formed at high coverage [9].

Ru/MgO was found to be a highly active catalyst for the reduction of NO by H_2 to N_2 [3,27]. On the other hand, ruthenium is a good catalyst for the ammonia production. The question is, how does ruthenium behave so differently in these reactions? In order to answer this question, the basic knowledge of the composition of the adsorption layers and of the surface processes such as reaction, adsorption, surface diffusion, etc. is necessary. As discussed in Ref. [3] the thermal desorption data from the Ru/MgO catalysis exhibited remarkable similarity to corresponding results obtained with the Ru(0001) single crystal under UHV. Therefore, the Ru(0001) single crystal may well serve as an adequate model system for Ru supported catalysts. The present paper focuses on the ex situ XPS study of the steady-state $\text{NO} + \text{H}_2$ reaction on the Ru(0001) surface at total pressure 10^{-4} Torr. The “low-pressure/single-crystal” results were compared with the finding for the Ru/MgO catalyst [3,27]. Since, the literature results deal mainly with low-temperature NO, adsorption of NO at 300 K on the Ru(0001) surface was studied as well. Also, XPS has several advantages compared to EELS and IRAS/RAIRS, which were employed before, because XPS provides quantitative and qualitative information on the surface composition and all adsorbed species (NO, N, NH_x , O) can be detected simultaneously.

2. Experimental

The experiments were carried out in the stainless steel chamber of the modified Leybold LHS 12 MCD system equipped with facilities for ultraviolet photoelectron spectroscopy (UPS), X-ray photoelectron spectroscopy (XPS) and ion scattering spectroscopy (ISS) (base pressure $\leq 10^{-10}$ mbar). The XPS data were obtained using the MgK_α radiation ($h\nu = 1253.6$ eV) and a fixed analyzer pass energy of 48 eV, corresponding to a resolution of 0.95 eV, which was measured as a full width at half maximum (FWHM) of the Ru3d_{5/2} peak. Binding energy (BE) was referred to the Fermi level and the linearity and slope were calibrated using the $\text{Au}4f_{7/2} = 84.0$ eV and $\text{Cu}2p_{3/2} =$

932.7 eV peaks. The Ru3d_{5/2} peak was set at a BE of 280.1 eV.

A Ru single crystal used in the experiments was oriented along the (0001) direction within $<0.5^\circ$. The single crystal was spot-welded between two tungsten wires and was heated resistively. The temperature of the single crystal was measured by means of a chromel–alumel thermocouple spot-welded to an edge of the crystal. The cleaning procedures included Ar^+ -etching followed by annealing cycles in oxygen and in vacuum, and flashing up to 1500 K in vacuum. The cleanliness of the sample was checked by XPS and UPS prior to each experiment.

Reaction and gas exposure were performed in the stainless steel preparation chamber (base pressure $\leq 1 \times 10^{-9}$ mbar). The sample was then transferred to the UHV analyzer chamber within ≈ 1 min. Gas exposures were measured in Langmuir (L), 1 L being 10^{-6} Torr s. Nitric oxide with a purity of 99.95% and high-purity (99.9999%) hydrogen, both supplied by Linde, were used for the experiments without further purification.

The coverage was measured in monolayer (ML) in respect of the number of ruthenium atoms in the topmost layer which for Ru(0001) equals to 1.58×10^{15} atoms cm^{-2} [9]. The concentrations of the chemical elements in the near-surface region were estimated after the subtraction of a Shirley type background, taking into account the corresponding atomic sensitivity factors [28]. The surface concentrations of the oxygen-containing species (NO_{ads} and O_{ads}) were estimated by measuring the ratio between the areas of the O 1s and Ru 3d_{5/2} peaks. The as-calculated value was then compared with the corresponding value for the oxygen saturation on the Ru(0001) surface. The saturated coverage was assumed to be equal to 0.5 ML [9].

3. Results

3.1. The adsorption of NO on the Ru(0001) surface

The studies of NO on the Ru(0001) surface [7–10, 12,14,18,21–24] mainly focused on the low-temperature adsorption when the well-ordered adsorption layers were formed. The diffusion ability of the species in such layers is supposed to be low and, therefore, the low-temperature systems cannot adequately represent the behaviour of the “real-world” ruthenium catalysts. In order to obtain some guidance for the conditions when the diffusion processes play an important role (see for instance [17]), we studied the adsorption of NO and O_2 on the Ru(0001) surface at room and elevated temperatures. The XPS results are summarised in Fig. 1.

The O_{ads} layer after exposure of the Ru(0001) surface to 100 L O_2 at 340 K showed a narrow peak at 529.8 eV in the O 1s region (Fig. 1(a)). The peak parameters such as the peak position, the intensity, the FWHM and the shape did not change as the adsorption temperature increased up to 400 K (spectra not shown here). Two well-resolved peaks in both the O 1s and N 1s regions (Fig. 1(b))

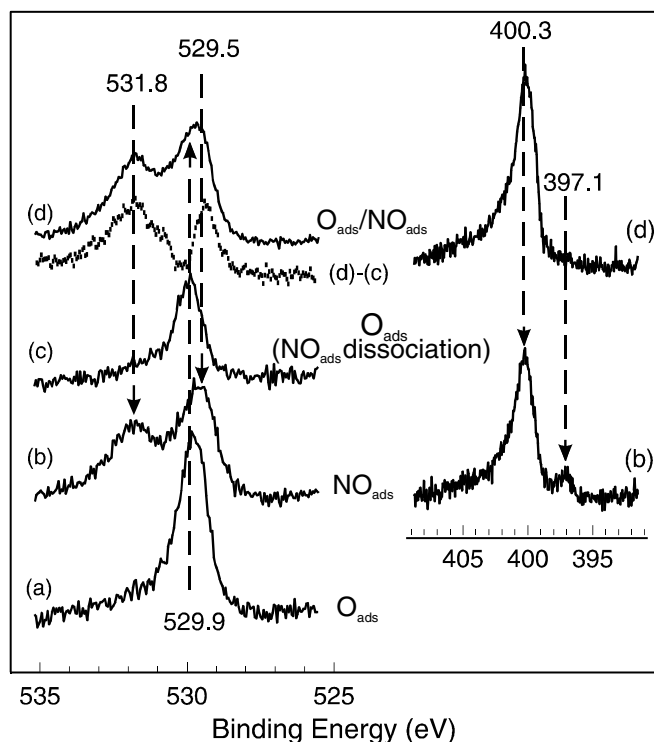


Fig. 1. O 1s and N 1s XP spectra obtained from (a) the O_{ads} layer (100 L O_2 at 340 K), (b) the saturated NO_{ads} layer (100 L NO at 300 K), (c) layer (b) heated in UHV at 700 K, (d) layer (c) exposed to 100 L NO at 300 K. The differential spectrum (d)–(c) is plotted as dots.

were obtained from the Ru(0001) surface exposed to NO up to saturation (100 L, 300 K). Peak assignments were performed based on the literature data summarised in Table 1. The two peaks at 400.3 and 397.1 eV in the N 1s core level spectra were assigned to molecularly adsorbed NO and N_{ads} , respectively [9,12]. We also observed the N 1s peak at 397.1 eV after saturating the Ru(0001) surface with N_{ads} by the decomposition of NH_3 . The presence of the N_{ads} species proved that NO dissociates during adsorption. The two molecular states of NO_{ads} , threefold-

Table 1
BE of O 1s and N 1s peaks of surface species formed by NO adsorption on the Ru(0001) surface

Species	O 1s BE (eV)	N 1s BE (eV)	References
v_1 - NO_{ads} the threefold position	530.3–530.7	399.6–399.9	[9,12,22,23]
v_2 - NO_{ads} the on-top position	531.8	400.0–400.1	[9,12,22,23]
O_{ads} (NO dissociation)	529.8–530.1	–	[9,12]
N_{ads} (NO dissociation)	–	396.9–397.3	[9,12]
v_1 - NO_{ads} the threefold position	529.4	400.4	This article
v_2 - NO_{ads} the on-top position	531.8	400.4	This article
O_{ads} (NO dissociation)	529.8–529.9	–	This article
N_{ads} (NO dissociation)	–	397.1	This article

bridge and on-top, could not be resolved in the N 1s core level spectra and, therefore, these states were characterised by the broad peak at 400.3 eV [9]. According to the literature [7,9,17], NO adlayer was supposed to be composed of the two molecular states, v_1 (threefold bridge) and v_2 (on-top), and the dissociation products: O_{ads} and N_{ads} . Two O 1s peaks at 529.7 and 531.8 eV were associated with these molecular NO_{ads} and O_{ads} species formed during NO dissociation. As seen in Table 1, the threefold coordinated NO_{ads} , v_1 , and O_{ads} are characterised by the overlapping O 1s peaks. The presence of O_{ads} on the surface was indirectly supported by the N 1s peak at 397.1 eV assigned to N_{ads} . Since the N_{ads} species was found and since the O_{ads} species was supposed to be more stable than N_{ads} [3,8,9,29], O_{ads} should remain on the surface after NO dissociation.

In order to distinguish between the molecular and dissociative states of NO_{ads} , a saturated NO_{ads} layer was heated in UHV to 700 K. According to the literature [8,9,29], heating leads to NO_{ads} decomposition and desorption; N_{ads} recombines and desorbs as N_2 ; O_{ads} remains on the surface. Indeed, as shown in Fig. 1(c), the XPS spectrum obtained after NO_{ads} layer heating showed a single peak at 529.9 eV, which was identical to those observed after O_2 adsorption (Fig. 1(a)). The only difference was that the coverage after O_2 adsorption was two times higher than the O_{ads} coverage after NO_{ads} decomposition.

Further exposure of $O_{\text{ads}}/Ru(0001)$, which was prepared through NO_{ads} thermal decomposition, to 100 L NO at 300 K restored the N 1s peak at 400.3 eV and the O 1s peaks at 529.5 (v_1) and 531.8 eV (v_2) as shown in Fig. 1(d). The absence of the N 1s peak at 397.1 eV showed that no dissociative adsorption of NO_{ads} occurred. So the O_{ads} species inhibited dissociation of nitric oxide but both the v_1 and v_2 molecular states of NO_{ads} were recovered. The total amount of NO_{ads} on the $O_{\text{ads}}/Ru(0001)$ surface decreased by 25% in comparison to the Ru(0001) surface. The amount of on-top coordinated NO_{ads} remained approximately constant, while the amount of threefold NO_{ads} decreased twofold. So, the presence of O_{ads} , which is presumably in the threefold-hollow coordination, inhibited NO adsorption in the threefold hollow site. Indeed, the similar effect was observed by TPD, when NO was over an oxygen-covered Ru(0001) [25]. First, at 2.3 L preadsorbed O_2 the amount of NO_{ads} that dissociates was reduced to 30%. Second, in the presence of pre-adsorbed O_{ads} , NO_{ads} desorbed in a single TPD peak corresponding to the v_2 state of NO_{ads} on a clean surface [25].

The thermal stability of the saturated NO_{ads} layer was studied by stepwise heating in UHV. The saturated NO_{ads} layer was prepared by exposure of 10 L NO on the Ru(0001) surface at room temperature. After each heating, the sample was cooled and the O 1s and N 1s core level spectra were accumulated at room temperature as shown in Fig. 2. The spectra were curve-fitted assuming a Doniac–Sunijc peak shape [30]. The O 1s region was fitted with three peaks at 529.5, 529.9 and 531.7 eV, whereas the

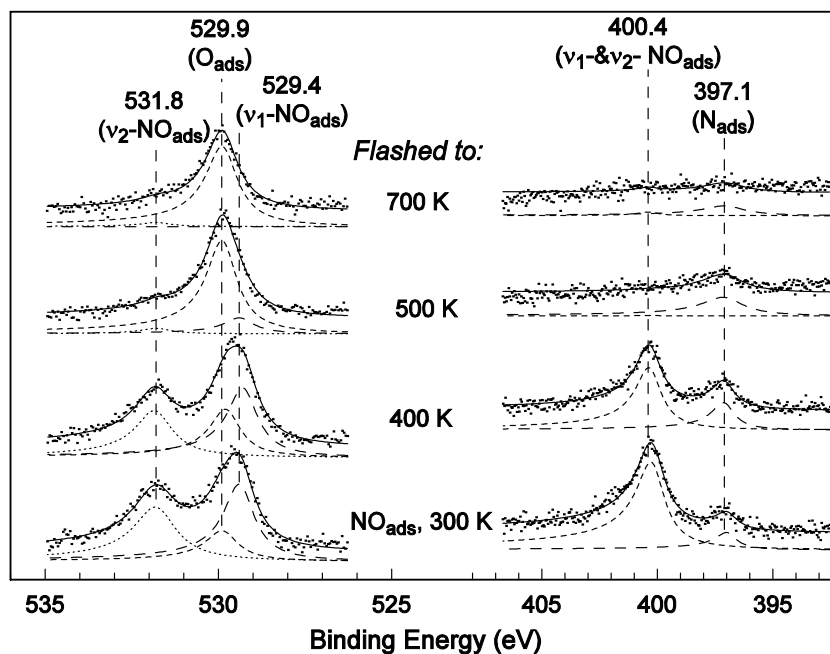


Fig. 2. Raw O 1s and N 1s XP spectra (dots) measured after saturating the Ru(0001) surface at 300 K with NO and after subsequent flashing to the given temperature in vacuum. The curve fit of the O 1s and N 1s lines was done assuming a Doniac–Sunijc peak shape.

N 1s core level spectra was described by two peaks at 397.1 and 400.4 eV (Fig. 2). The oxygen peaks were assigned based on the discussion above and the literature data [7,9,17]: the peaks at 529.5 and 531.7 eV were assigned to threefold, v_1 , and on-top, v_2 , coordinated NO_{ads} respectively; the peak at 529.9 eV was attributed to O_{ads} . The N 1s peaks at 397.1 and 400.4 eV were the features of N_{ads} and the molecular states of NO_{ads} , respectively. The coverage of the adsorbed species as a function of temperature is shown in Fig. 3. NO dissociation at RT led to an O_{ads} concentration that was slightly higher than the corresponding number for N_{ads} . Then, the coverage of NO dissociation products, O_{ads} and N_{ads} , increased with temperature. As shown in Fig. 3, the N_{ads} coverage passed through a maximum at 400 K and then dropped to zero. The coverage of O_{ads} demonstrated a steady growth up to 500 K and then remained unchanged. The growth of O_{ads} coverage correlated well with decreasing NO_{ads} coverage, reflecting dissociation and desorption of nitric oxide. NO_{ads} desorption/dissociation finished after heating at 500 K.

3.2. The reduction of NO with H_2 on the Ru(0001) surface

The reaction between NO and H_2 was studied both on the originally clean Ru(0001) surface and the oxygen-covered surface at 320 and 390 K. These temperatures corresponded to the NO conversion of 50% and 100%, respectively [27]. Prior to each XPS measurement, Ru(0001) was treated for 10 min in a 30:1 mixture of H_2 and NO (total pressure = 10^{-4} mbar) in the preparation chamber. The reaction mixture was pumped out and then

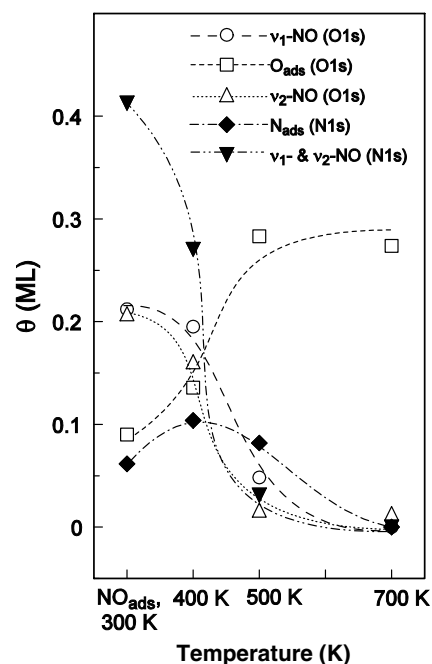


Fig. 3. The coverage of the adsorbed species as a function of the flashing temperature, the calculations were done basing on the results of the curve fit analysis.

the crystal was cooled to 320 K and transferred to the analysis chamber within 1 min.

Fig. 4 shows the O 1s and N 1s spectra measured after the steady-state reaction at 390 K on the originally clean Ru(0001) surface. The molecularly adsorbed NO in the linear on-top (531.7 eV) and threefold (529.4 eV) positions were found on the surface after the reaction. Since the

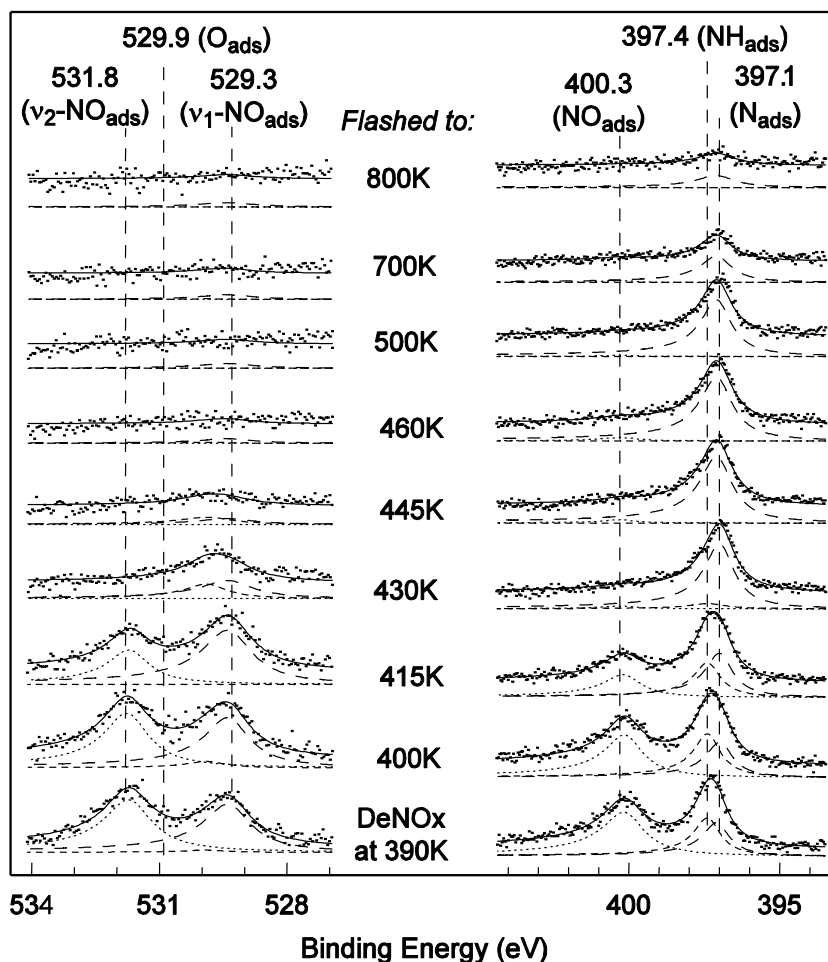


Fig. 4. Raw O 1s and N 1s XP spectra (dots) taken after exposure of the clean Ru(0001) surface to a 30:1 mixture of H₂ and NO (total pressure = 10⁻⁴ mbar) at 390 K for 10 min and after heating the as-prepared adlayer stepwise under vacuum. The curve fit of the O 1s and N 1s lines was done assuming a Doniac–Sunjic peak shape.

FWHM of the peaks was approximately 1 eV, the existence of the peak at 529.9 eV due to O_{ads} could be unambiguously ruled out. One can conclude that no O_{ads} was on the surface after the reaction. Two peaks at 400.4 and 397.4 eV were observed in the N 1s core level spectra. The peaks at 400.4 eV could be unambiguously assigned to NO_{ads}. The peak at 397.4 eV was slightly shifted towards higher BE in comparison to the N_{ads} peak at 397.1 eV. Also, the peak at 397.4 eV was found to be broader than the N_{ads} peak, therefore, this peak was tentatively assigned to a N-containing species other than NO_{ads} and N_{ads}.

We observed the peak at 397.4 eV during NH₃ decomposition on the Ru(0001) surface and assigned it to adsorbed NH fragments. This assignment was in agreement with all the available literature data summarised in Table 2. Unfortunately, not much XPS data on NH_x fragments with clear assignment of the peak positions were available in the literature (Table 2). Sun et al. [31] and Weststrate et al. [32] reported the BE of 397.5 eV and 397.6 eV for the NH_{ads} species on the Pt(111) and Ir(110) surfaces, respectively. Assuming the correctness of the above out-

Table 2

Core level BE values of N-containing species adsorbed on different surfaces

Sample	BE (eV)				Reference
	NH _{3,ads}	NH _{2,ads}	NH _{ads}	N _{ads}	
Fe(poly)	400.0				[37]
Fe(110), (111)	400.0		397.3	396.6–397.0	[38]
Al(poly)	400.0	399.4	398.0	397.0	[39]
Amorphous Si	400.1	398.6	398.0	397.4	[40]
GaAs(110)	400.1	398.5			[41]
Pt(111)	399.3	397.5	397.5		[31]
Ir(110)	399.5–400.1		397.6	396.5	[32,42]
Ru(0001), (1110)	400.0	398.1	397.5–397.6	397.1–397.3	[12]
Ru(0001)			397.4	397.1	This work

lined BE assignments, we suggested that the NH_{ads} species was present on the Ru(0001) surface during the steady-state catalytic reduction of nitric oxide with excess hydrogen. The other adsorbed species were molecularly on-top and bridge coordinated NO_{ads} and probably N_{ads}.

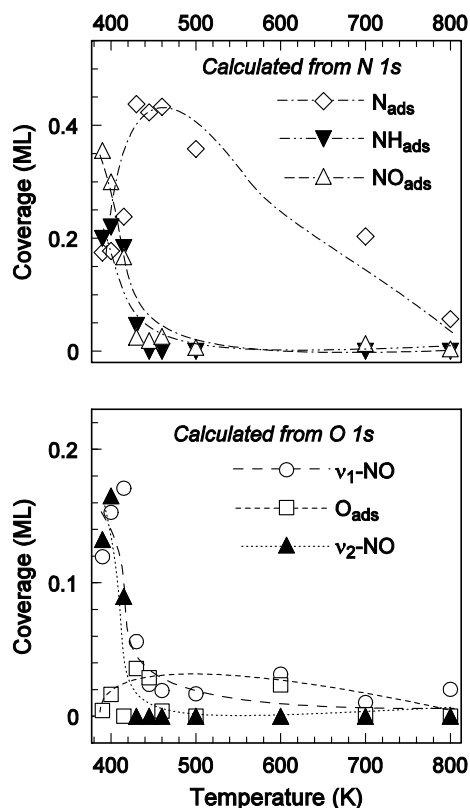


Fig. 5. The coverage of the adsorbates on the treated surface as a function of flashing temperature (see treatment conditions in the caption of Fig. 4). The calculations were done basing on the results of the curve fit analysis.

In order to identify the surface species, the Ru(0001) surface was heated after treatment in the reaction mixture at 390 K for 10 min in vacuum. The XPS spectra were collected at room temperature as shown in Fig. 4. The coverage of the adsorbed species as a function of temperature is shown in Fig. 5. The adlayer did not change up to 415 K. But after heating at 430 K, dramatic changes were observed. First, the O 1s peak at 531.7 eV, which is a characteristic of the on-top coordinated NO_{ads} species, v_2 , disappeared. Second, the peak at 529.5 eV, which was assigned to the threefold coordinated NO_{ads} species, v_1 , shifted to 529.7 eV. This reflected the appearance of O_{ads} . Simultaneously, the N 1s peak at 400.4 eV, which is a fingerprint of molecularly adsorbed states of NO, v_1 and v_2 , also disappeared. This pointed to dissociation and/or desorption of NO_{ads} . The threefold coordinated NO_{ads} showed a slightly higher thermal stability in comparison to the linearly coordinated form (Fig. 5). Therefore, the threefold coordinated NO_{ads} species was supposed to be an intermediate for NO dissociation: due to dissociation, the threefold NO_{ads} might get depleted but the linear form converts into the threefold NO_{ads} . The appearance of O_{ads} coincided with the low-BE shift of the N 1s peak from 397.4 eV to 397.1 eV. This shift cannot be explained by a technique artefact because no deviation was observed for the other peaks in particularly for the Ru3d_{5/2} peak. Also, the low-BE shift of the N 1s peak was consistent during

numerous heating experiments. Therefore, the low-BE shift could be assigned to the transformation of NH_{ads} into the N_{ads} species.

All oxygen-containing species disappeared after heating at 445 K. On the other hand, the adsorbed nitrogen was detected even after heating to 800 K. It is remarkable that in the presence of co-adsorbed atomic oxygen, the full desorption of all nitrogen-containing species was achieved by heating below 700 K (compare with Fig. 2). The conclusion could be drawn that O_{ads} essentially destabilises the co-adsorbed N_{ads} . This conclusion is a good agreement with the TPD data reported in Ref. [25]. There it was found that N_2 forms between 600 K and 800 K when a NO_{ads} layer was heated in the presence of H_2 , whereas heating of a NO_{ads} layer in vacuum led to N_2 desorption between 400 K and 600 K. This finding corroborates the hypothesis about the repulsive interaction effect of O_{ads} on N_{ads} .

The O-containing species disappeared already at temperatures as low as 445 K and this could not be due to oxygen desorption. As shown in Fig. 2, oxygen remained on the surface after heating to 700 K. Heating above 1100 K is required to remove oxygen. O_{ads} was supposed to be consumed in the course of the reaction with hydrogen-containing species. As shown in Fig. 4, the O-containing species disappear simultaneously with the consumption of the NH_{ads} species and the formation of N_{ads} . This fact unambiguously pointed to the reaction between O_{ads} and NH_{ads} . Water formed during this reaction should desorb immediately because the temperature was too high for the H_2O and OH adsorption. This was consistent with the fact that no new peaks appeared in the O 1s region by XPS or in the valence zone by UPS.

The Ru(0001) surface was examined after steady-state $\text{NO} + \text{H}_2$ reaction at 320 K. Fig. 6 shows the O 1s and N 1s core level spectra obtained from the Ru(0001) surface after the reaction for 10 min at 320 and 390 K. The overall surface coverage was higher at the low reaction temperature. The change of the reaction temperature altered the relative concentration of the N-containing adsorbed species. At 320 K, where the conversion of NO was 50% for a Ru/MgO catalyst [27], the most abundant surface species was molecularly adsorbed NO (mainly in the threefold coordinated form) and the concentration of N_{ads} was low. At 390 K, where the conversion of NO was 100% for a Ru/MgO catalyst [27], the coverage of N_{ads} increased to a value comparable to the coverage of the NH_{ads} species, whereas θ_{NO} reduced by almost 30%.

Finally, in order to clarify the effect of adsorbed oxygen, the reaction was also studied under the same experimental conditions at 390 K. The oxygen-covered surface was prepared by dosing 10 L NO at room temperature and flashing to 700 K to remove all N-containing species as discussed in Section 3.1. The initial presence of adsorbed oxygen on the surface did not seem to affect the reaction. The composition of the adlayer after the reaction both on the initially adsorbate-free and on the oxygen-covered surfaces was qualitatively and quantitatively the same (spectra not shown here).

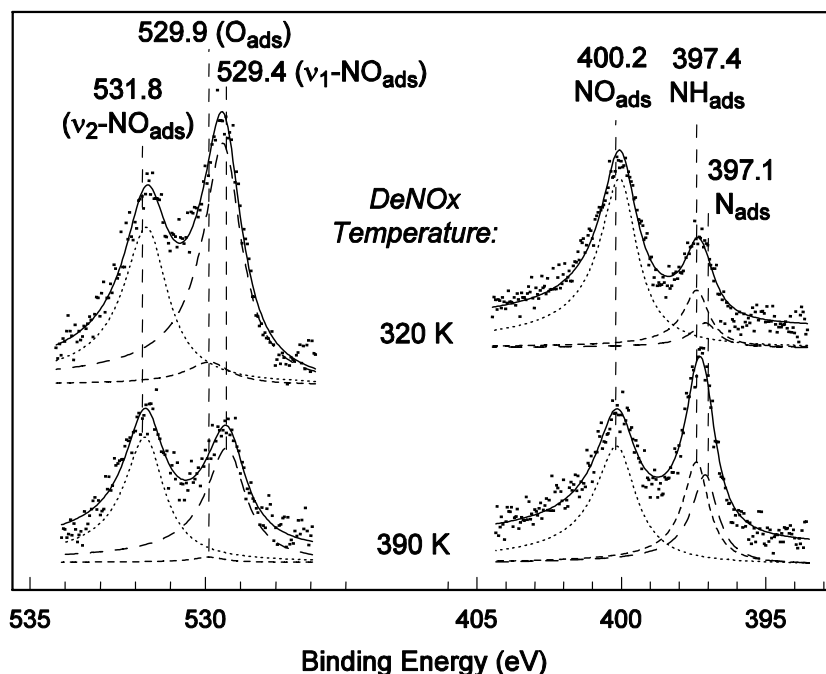


Fig. 6. O 1s and N 1s XP spectra taken after exposure of the clean Ru(0001) surface to a 30:1 mixture of H₂ and NO (total pressure = 10⁻⁴ mbar) at 320 K and 390 K for 10 min.

4. Discussion

4.1. NO adsorption

As seen in Fig. 1, 0.25 ML pre-adsorbed oxygen is sufficient to block NO_{ads} dissociation at RT completely. On the Ru(0001) surface at 300 K, NO dissociates predominantly at atomic steps to which the NO_{ads} species migrate and from where the generated N_{ads} and O_{ads} atoms diffuse away [17]. However, O_{ads} atoms may remain attached with the step sites and, thus, may cause inhibition of the “active sites”. The XPS results demonstrate that O_{ads} coverage after NO adsorption was slightly higher than the corresponding value for N_{ads}. The N_{ads} species formed during NO dissociation was supposed to recombine and desorb as N₂. This is in a good agreement with the data obtained from the Ru/MgO catalysis [3,27]. Thus, the partial recombination of N_{ads} followed by N₂ desorption was found during an exposure of the Ru/MgO catalysis to NO at room temperature by applying frontal chromatography [3]. However, the comparison between a Ru(0001) single crystal and a Ru/MgO catalysis can be only qualitative because the density of defect sites on the well-ordered surface of a Ru(0001) single crystal is much lower than the corresponding value for the 200 Å supported Ru particles [3].

Our experiments demonstrated the destabilisation effect of the O_{ads} species on N_{ads}. On the O-free surface, N_{ads} was observed after heating at 800 K (Figs. 4 and 5), whereas only a little of N_{ads} was found on the O-containing surface after heating at 500 K (Figs. 2 and 3). Nagl et al. [20] reported that there is a phase equilibrium in the mixed N_{ads} and O_{ads} layer between the two-component 2 × 2 patches

and its dilute gas phase, i.e., an O-rich dense phase and N-rich lattice gas. Due to relatively weak N–O interaction in the dense phase, the enthalpy of the mixing is positive, therefore, the growth of 2 × 2 dense phase causes two-dimensional “vapour pressure” increases and N atoms might start to recombine and leave the surface.

According to HREELS data [7,8], at 150 K at low coverage, NO_{ads} adsorbs only in the threefold coordinated adsorption states on the steps, v₀, and on the terraces, v₁. These states dissociated completely upon heating in UHV at 250–310 K. Since no new state formed upon heating, the threefold coordinated states were supposed to be an intermediate species for NO dissociation. Thomas and Weinberg [7] reported that at high coverage the threefold NO_{ads} decomposed first and only then the linearly coordinated species dissociated. The hypothesis about the threefold coordinated NO_{ads} as an intermediate for dissociation agrees with a quantum-mechanic modelling predicting a higher value of the π back donation to the anti-bonding molecular orbital of NO_{ads} for the threefold coordinated species [21]. It is remarkable that an N–O bond length of the linearly coordinated NO_{ads}, v₂, was calculated to be equal 1.20 ± 0.01 Å and 1.13 ± 0.06 Å from NEXAFS spectra [14] and from LEED-IV data [19,22] respectively, whereas N–O bond in the threefold coordination, v₁, was elongated to 1.32 ± 0.02/1.28 ± 0.02 Å (NEXAFS) [14] and 1.24 ± 0.07/1.22 ± 0.06 Å (LEED-IV) [19,22]. The N–O bond in the threefold state elongates in comparison to in the linearly coordinated form due to a substantially stronger π back donation [21]. The π back donation should result in weakening the N–O bond. Therefore, this also points to the higher ability of NO to dissoci-

ate in the threefold state. The indirect experimental proof observed by us is that the presence of O_{ads} , which is presumably in the threefold-hollow coordination, inhibited NO adsorption in the threefold hollow coordination and no dissociation of NO_{ads} was found (Fig. 1).

In our heating experiments, the threefold and linearly coordinated NO_{ads} species decomposed almost simultaneously. However, this does not contradict the hypothesis about the threefold coordinated NO_{ads} as an intermediate for NO dissociation. This fact underlines the importance of the surface diffusion. At room temperature the diffusion is fast enough (i) to clean the “active sites” from the product of dissociation and (ii) to bring a new portion of a reagent. This is not the case at low temperatures where the dissociation products remain where they formed and the adsorption layer could not be mixed by diffusion.

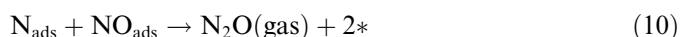
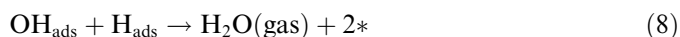
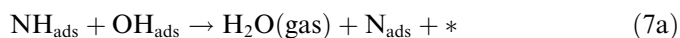
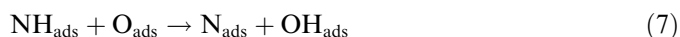
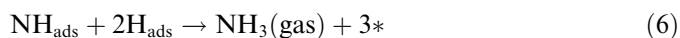
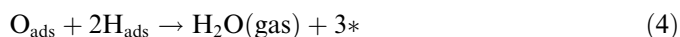
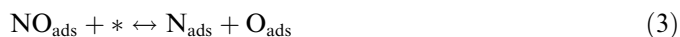
4.2. $NO + H_2$ reaction

The catalytic reduction of NO with H_2 on ruthenium is a process with an extremely high selectivity to N_2 , whereby less than 1% of the fed NO is converted into NH_3 at 100% conversion (see Ref. [3] and references therein). On the other hand, ruthenium is a highly active catalyst for the synthesis of ammonia from nitrogen and hydrogen (see Ref. [33] and references therein). Moreover, it has been proven that the first hydrogenation step of N_{ads} to NH_{ads} is the rate-determining step of ammonisation in co-adsorbed $N_{\text{ads}}/H_{\text{ads}}$ layers [34]. Is the formation of the NH_{ads} species observed in the present in contradiction with the already mentioned high selectivity to N_2 in the selective catalytic reduction of NO?

One of the main questions on this issue is the reliability of the assignment of the NH_{ads} species. The XPS data unambiguously demonstrated (Fig. 4) that the Ru(0001) surface after exposure to a reaction mixture at 390 K did not contain O_{ads} . Moreover, the heating of this surface did not lead to O_{ads} formation and the curve fitting gave no indication of any 529.9 eV peak. O_{ads} does not desorb from the Ru(0001) surface at discussed temperature. The only reasonable explanation for the “missing” of O_{ads} could be the reaction to form water. So, some source of hydrogen must exist on the surface after the reaction. H_{ads} can be ruled out because according to the literature [35], hydrogen does not adsorb at 300 K on the surface covered by N_{ads} . Therefore, the only possible source of hydrogen could be NH_x species. According to the literature data in Table 2, the N 1s peak from $NH_{3,\text{ads}}$ and $NH_{2,\text{ads}}$ are expected between 397.5 eV and 400 eV. In our experiments, the peak at 397.4 eV was observed. The rule of thumb is that the ΔBE between different $NH_{x,\text{ads}}$ species is approximately 1 eV (see for instance Refs. [31,32] and Table 2). From this point of view, the ΔBE between NH_{ads} (397.4 eV) and N_{ads} (397.1 eV), which is only 0.3 eV, does not look very convincing. On the other hand, the higher BE shift of the N 1s and decrease of its FWHM were repeatedly observed during all heating of the surface after

the reaction. The analysis was hindered by the presence of the N_{ads} species resulting in the peak at 397.1 eV. However, the curve-fitting performed with the several experimental sets applying the same fitting parameters unambiguously pointed to the two components at 397.4 eV and 397.1 eV. Also, since the peak splitting is small, the peak at 397.4 eV obviously cannot be assigned to $NH_{2,\text{ads}}$ species. The vast nature of the experimental data along with the literature allowed us safely to assume the presence of the NH_{ads} species on the surface after the reaction.

The other question concerns the role of the NH_{ads} species in the reaction mechanism. The following simple reaction mechanism can be suggested.



Here * denotes a vacant site on the surface. We do not distinguish the types of active sites, which can vary for the different reaction steps. However, even this primitive mechanism is able to explain peculiarities of $NO + H_2$ reaction. The NH_{ads} species can be an intermediate for ammonia (step (6)). NH_{ads} oxidation by OH group was also included (7a). The similar reaction step was proposed by van den Broek et al. [36] in the case of ammonia oxidation on platinum and iridium. The hydrogenation of NH_{ads} to NH_3 can be kinetically limited due to low H_{ads} coverage in the presence of N_{ads} as discussed above (see Ref. [35]). $NH_{2,\text{ads}}$ which could be formed from the NH_{ads} species, likely is not stable and cannot be detected. The curve-fitting analysis of the XPS spectra after reaction did not show a component between 398 eV and 399 eV. So, NH_{ads} could be involved in N_2 formation through steps (7) and (7a).

The indirect proof of the kinetic limitation of NH_{ads} in the hydrogenation to NH_3 was found during the microkinetic investigation of NO reduction on MgO-supported ruthenium catalysts [3]. It was observed that the high selectivity to N_2 strongly depends on the catalyst surface coverage in the following way: at high coverage, the presence of adsorbed NO and of its dissociation products shifts the dissociative adsorption equilibrium of H_2 , thus hindering the full hydrogenation of adsorbed nitrogen to ammonia; as soon as the surface coverage lowers and sufficient H_{ads} species are available, the main product will be NH_3 . This is

consistent with the conclusions made above. According to the XPS results, after the reaction the surface was covered with NO_{ads} , N_{ads} and NH_{ads} . Therefore hydrogen coverage should be low and NH_{ads} hydrogenation to NH_3 should be hindered (step (6)).

The XPS data (Fig. 6) showed that NO_{ads} coverage after the reaction at 320 K was higher than the corresponding values after the reaction at 390 K but the amount of N_{ads} and NH_{ads} was less than at 390 K. Also the threefold NO_{ads} was the dominating species at 320 K. On the Ru/MgO catalyst [27], the temperatures of 320 K and 390 K corresponded to 50% and 100% NO conversions, respectively. These two facts are reasonably consistent. So, high NO coverage might cause decreased NO conversion through inhibition of NO_{ads} dissociation due to the absent of vacant sites (step (3)). This might indicate that NO_{ads} dissociation might be the rate-determining step.

De Wolf et al. [25] reported about poisoning the Ru surface by O_{ads} during $\text{NO} + \text{H}_{\text{ads}}$ reaction. This effect was not detected in the present study. The surface composition after the reaction on the surface deliberately covered with O_{ads} was identically those after the reaction on the originally clean surface. The XPS technique also did not find O_{ads} species. The disagreement with Ref. [25] could be explained by different reaction conditions used in our experiments.

5. Conclusions

The investigation of the adsorption of NO at room temperature showed, in agreement with the literature, that NO partially dissociated on the Ru(0001) surface already at room temperature, whereas the major fraction was molecularly adsorbed. Two different states (on-top and threefold coordinated) of adsorbed NO could be distinguished. Dissociation of NO_{ads} was suggested to occur through the formation of the threefold coordinated NO species. The strong destabilisation of adsorbed nitrogen by the presence of co-adsorbed oxygen was observed.

After steady-state NO reduction, the adsorption layer consisted of molecular NO both linearly and bridge coordinated, NH_{ads} and N_{ads} species, which relative concentrations depended on the reaction temperature. The coverage of the NH_{ads} and N_{ads} species was higher after the reaction at 390 K than the corresponding values for the reaction at 320 K. NO dissociation was supposed to be a rate-determining step. The NH_{ads} species might be involved in the mechanism of N_2 formation.

Acknowledgements

One of us (D.Z.) gratefully acknowledges receipt of an Alfred Toepfer Stiftung F.V.S. Fellowship and a Max-Planck-Gesellschaft Fellowship. D.Z. also greatly appreciates the hospitality of Prof. Robert Schlögl and helpful discussion with him during performing the experiments. The authors appreciate the kind help of Professor Kieran

Hodnett for revising the manuscript. The authors would like to thank Michael Wesemann for software development for an XPS and UPS analysis.

References

- [1] A. Ozaki, K. Aika, Catal. Sci. Technol. 1 (1981) 87.
- [2] B.G. Mandelik, J.R. Cassata, P.J. Shires, C.P. Van Dijk, US Patent 4568530, 1986, (Kellogg, M. W., Co., USA).
- [3] A. Hornung, M. Muhler, G. Ertl, Catal. Lett. 53 (1998) 77.
- [4] A. Hornung, M. Muhler, G. Ertl, Top. Catal. 11/12 (2000) 263.
- [5] H. Abrevaya, M.J. Cohn, W.M. Targos, H.J. Robota, Catal. Lett. 7 (1990) 183.
- [6] G.C. Bond, J.C. Slaat, J. Mol. Catal. 89 (1994) 221.
- [7] G.E. Thomas, W.H. Weinberg, Phys. Rev. Lett. 41 (1978) 1181.
- [8] P.A. Thiel, W.H. Weinberg, J.T. Yates Jr., Chem. Phys. Lett. 67 (1979) 403.
- [9] E. Umbach, S. Kulkarni, P. Feulner, D. Menzel, Surf. Sci. 88 (1979) 65.
- [10] P. Feulner, S. Kulkarni, E. Umbach, D. Menzel, Surf. Sci. 99 (1980) 489.
- [11] P.A. Thiel, W.H. Weinberg, J. Chem. Phys. 73 (1980) 4081.
- [12] C. Egawa, S. Naito, K. Tamaru, Surf. Sci. 138 (1984) 279.
- [13] K.M. Neyman, N. Roesch, K.L. Kostov, P. Jakob, D. Menzel, J. Chem. Phys. 100 (1994) 2310.
- [14] F. Esch, S. Ladas, S. Kennou, A. Siokou, R. Imbihl, Surf. Sci. 355 (1996) L253.
- [15] J. Trost, T. Zambelli, J. Wintterlin, G. Ertl, Phys. Rev. B: Condens. Matter 54 (1996) 17850.
- [16] T. Zambelli, J. Trost, J. Wintterlin, G. Ertl, Phys. Rev. Lett. 76 (1996) 795.
- [17] T. Zambelli, J. Wintterlin, J. Trost, G. Ertl, Science (Washington, DC) 273 (1996) 1688.
- [18] P. Jakob, M. Stichler, D. Menzel, Surf. Sci. 370 (1997) L185.
- [19] M. Stichler, D. Menzel, Surf. Sci. 391 (1997) 47.
- [20] C. Nagl, R. Schuster, S. Renisch, G. Ertl, Phys. Rev. Lett. 81 (1998) 3483.
- [21] M. Staufer, U. Birkenheuer, T. Belling, F. Nortemann, N. Rosch, M. Stichler, C. Keller, W. Wurth, D. Menzel, L.G.M. Pettersson, A. Fohlisch, A. Nilsson, J. Chem. Phys. 111 (1999) 4704.
- [22] M. Stichler, D. Menzel, Surf. Sci. 419 (1999) 272.
- [23] M. Stichler, C. Keller, C. Heske, M. Staufer, U. Birkenheuer, N. Rosch, W. Wurth, D. Menzel, Surf. Sci. 448 (2000) 164.
- [24] T. Nishida, C. Egawa, S. Naito, K. Tamaru, J. Chem. Soc., Faraday Trans. 1 (80) (1984) 1567.
- [25] C.A. de Wolf, M.O. Hattink, B.E. Nieuwenhuys, J. Phys. Chem. B 104 (2000) 3204.
- [26] G. Blyholder, J. Phys. Chem. 68 (1964) 2772.
- [27] A. Hornung, Ph.D. Thesis, Freie Universität, 1998.
- [28] J.J. Yeh, I. Lindau, At. Data Nucl. Data Tables 32 (1985) 1.
- [29] G.E. Thomas, W.H. Weinberg, Div. Chem. Chem. Eng., California Inst. Technol., Pasadena, CA, USA, 1978, p. 97.
- [30] S. Doniach, M. Sunjic, J. Phys. C 3 (1970) 285.
- [31] Y.M. Sun, D. Sloan, H. Ihm, J.M. White, J. Vac. Sci. Technol. A: Vac. Surf. Films 14 (1996) 1516.
- [32] C.J. Weststrate, J.W. Bakker, E.D.L. Rienks, S. Lizzit, L. Petaccia, A. Baraldi, C.P. Vinod, B.E. Nieuwenhuys, J. Chem. Phys. 122 (2005) 184705/1.
- [33] F. Rosowski, A. Hornung, O. Hinrichsen, D. Herein, M. Muhler, G. Ertl, Appl. Catal. A 151 (1997) 443.
- [34] O. Hinrichsen, F. Rosowski, A. Hornung, M. Muhler, G. Ertl, J. Catal. 165 (1997) 33.
- [35] D.C. Seets, M.C. Wheeler, C.B. Mullins, J. Chem. Phys. 103 (1995) 10399.
- [36] A.C.M. van den Broek, J. van Grondelle, R.A. van Santen, J. Catal. 185 (1999) 297.
- [37] K. Kishi, M.W. Roberts, Surf. Sci. 62 (1977) 252.

- [38] M. Grunze, Surf. Sci. 81 (1978) 603.
- [39] D.W. Johnson, M.W. Roberts, J. Electron Spectrosc. Relat. Phenom. 19 (1980) 185.
- [40] J.L. Bischoff, F. Lutz, D. Bolmont, L. Kubler, Surf. Sci. 251–252 (1991) 170.
- [41] X.Y. Zhu, M. Wolf, T. Huett, J.M. White, J. Chem. Phys. 97 (1992) 5856.
- [42] C.A. deWolf, J.W. Bakker, P.T. Wouda, B.E. Nieuwenhuys, A. Baraldi, S. Lizzit, M. Kiskinova, J. Phys. Chem. B 105 (2001) 4254.